POLITECNICO
MILANO 1863

DIPARTIMENTO DI MECCANICA

mecc

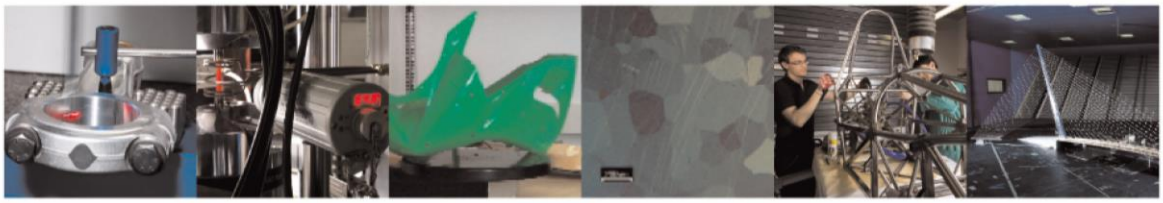

Condition Monitoring Of Railway Axles Based On Low Frequency Vibrations

Paweł Rolek, Stefano Bruni, Michele Carboni

This is a post-peer-review, pre-copyedit version of an article published in International Journal of Fatigue. The final authenticated version is available online at:
http://dx.doi.org/10.1016/j.ijfatigue.2015.07.004

This content is provided under CC BY-NC-ND 4.0 license

DIPARTIMENTO DI MECCANICA ■ POLITECNICO DI MILANO
via G. La Masa, 1 ■ 20156 Milano ■ EMAIL (PEC): pecmecc@cert.polimi.it
http://www.mecc.polimi.it
Rev. 0

CONDITION MONITORING OF RAILWAY AXLES BASED ON LOW FREQUENCY VIBRATIONS

Paweł ROLEK, Stefano BRUNI[1], Michele CARBONI

Department Mechanical Engineering, Politecnico di Milano

Via La Masa 1, 20156 Milano, Italy

Abstract

Railway axles are safety-critical components and their structural integrity needs to be properly monitored against potentially catastrophic failures. This paper proposes a method for the continuous condition monitoring of railway axles by measuring the axle in-service bending vibration and diagnosing the presence of a fatigue crack based on the examination of harmonic components with periodicity corresponding to an integer sub-multiple of the axle revolution period (*n*xRev).

To analyse the feasibility of the proposed method, full-scale measurements were performed on cracked and non-cracked railway axles undergoing fatigue tests and a mathematical Finite Element (FE) model of a cracked railway axle was defined and used to reproduce the laboratory experiments and also to analyse the case of a railway wheelset with cracked axle rolling on a railway track.

The results of both experimental and numerical investigations show that the 1xRev, 2xRev and 3xRev components of axle bending vibration can be used to detect the presence of cracks in axles, provided the crack area is in the range of 16% of axle cross section or larger. Hence, the proposed method cannot replace periodical non-destructive inspections, but may serve as an additional safety measure detecting cracked axles in an advanced stage of the damage process but still on time to avoid in-service failures.

Keywords: structural health monitoring, railway axles, low frequency vibrations

[1] Corresponding author: Tel.: +39-02-23998495, Fax: +39-02-23998492, E-mail: stefano.bruni@polimi.it.

1. Introduction

In railway vehicles, wheels are often used in pairs connected by an axle, this assembly being called the “wheelset”. Wheelsets are a very important subsystem in the vehicle, as they provide the interface with the track, support static and dynamic loads, provide traction, braking and guidance, the latter being the ability of the vehicle to follow the track [1]. Due to their very long service life (30 years or even more on European lines), railway wheelsets, and especially their axle, are prone to fatigue damage, which can be triggered by initial material defects or by service-related damage such as corrosion [2]-[3] or impacts with ballast stones [4]. The consequences of a fatigue failure occurring in a railway axle may be catastrophic, as the failure of one axle is likely to produce the derailment of the entire vehicle, which may in turn cause serious damage to the rolling stock and the infrastructure, injury of passengers and, in the worst case, even lead to fatalities.

To prevent fatigue failures in railway axles, the traditional design [5]-[6] based on the fatigue limit is complemented by a damage tolerant approach [7]-[9], where non-destructive testing (NDT) inspections are periodically performed on railway axles, typically using ultrasonic testing (UT) and magnetic particles testing (MT) techniques in combination [9]. However, despite the high standards of present engineering practice in NDT inspection, fatigue-induced axle failures still occasionally occur, representing a serious threat to the safe operation of railway systems [2]. A way to further reduce and possibly eliminate in-service failure is to implement continuous on-board structural health monitoring (SHM) of railway axles. In the technical literature, few initial investigations of possible strategies for continuous SHM of railway axles can be traced. One proposed solution is to extend the standard ultrasonic inspection methods so that they can be applied to a railway axle moving at service speed [10], but this requires the use of a very complicated wayside measuring equipment and the actual reliability of the SHM system has not been proved yet. Alternatively, the suitability of acoustic emission to detect cracked axles has been investigated [11]-[13], but a

number of practical issues remain to be addressed before the feasibility of this method for practical use can be demonstrated.

In this paper, a method for the continuous structural health monitoring of railway axles is proposed based on measuring the axle in-service bending vibration. Indeed, the presence of a crack perturbs the axi-symmetric bending stiffness of the axle, affecting the bending vibration at frequencies that are multiple integers of the frequency of revolution, referred to as *n*xRev in this paper. This SHM strategy entails the measure of harmonic components of axle bending vibration occurring in the low frequency region (below 200-300 Hz), therefore allows the use of a relatively simple, robust and inexpensive measuring set-up. It should be made clear however that, in order to produce a significant alteration of the *n*xRev axle enabling fault detection, the size of the crack must be relatively large (as will be shown later, the crack area should be in the range of 16% of axle cross section or larger). Therefore, the SHM application proposed here is not meant to replace NDT inspection, but to serve as an additional safety measure that aims at detecting cracked axles in an advanced stage of the damage process, but still on time to avoid a catastrophic failure. The research reported in this paper was partly performed in the framework of the SUSTRAIL project [14], funded by the European Commission under FP7.

The method investigated in this paper takes inspiration from previous research performed in the field of rotordynamics and condition monitoring of rotating shafts. For these systems, the so-called "crack breathing" mechanism is known to produce typical signatures in the spectrum of bending vibration that can be used to detect the presence of a crack, locate the crack along the shaft and provide an estimate of the crack size [15]-[18]. When these methods are applied to a railway axle however, significant additional issues need to be addressed, mainly because railway axles are rotating at speeds well below their first critical speed, whereas shafts in turbomachinery and other industrial machinery are often working above at least the first critical speed. Furthermore, heavy disturbance caused by wheel-rail contact in presence of track irregularity and wheel out-of-roundness needs to be faced.

To analyse the feasibility of the crack detection method proposed in this paper, full-scale fatigue (durability) experiments were performed on railway axles in the lab and a Finite Element (FE) model of a cracked railway axle was defined and used to reproduce them and to analyse the case of a railway wheelset with cracked axle rolling on a railway track.

The paper is organised as follows: in Section 2, the mechanism of crack-induced vibration in a rotating axle is introduced. In Section 3, full-scale laboratory experiments are described, providing experimental evidence of the relationship between the existence of a propagating crack in the axle and the occurrence of additional *n*xRev vibration. In Section 4, a non-linear FE model of a cracked axle reproducing the crack breathing mechanism is introduced and numerical results are presented for two different scenarios: first, the laboratory test scenario is considered and numerical results are compared to laboratory measurement. Then, the scenario of a wheelset running on a railway track is considered, including disturbance arising from geometrical imperfections in the track and in the wheels, in order to perform a preliminary analysis of the suitability of the proposed SHM methodology in view of its real application.

2. Crack-induced vibrations in a rotating axle

The presence of a crack in a rotating axle affects its bending vibration under several aspects. Firstly, it causes a local change in the bending stiffness affecting the amplitude of forced vibration as well as the system's natural frequencies and modes of vibration. If the axle is statically loaded, the presence of a crack increases the axle's static bow and results in the amplification of the 1xRev vibration component, i.e. synchronous with the revolution of the axle. Secondly, the crack perturbs the axi-symmetric behaviour in bending of the axle (Fig. 1a). When the rotating axle is subjected to bending along a fixed direction, as caused e.g. by gravitational loads, its static deflection changes with the angle of rotation, giving rise to bending vibration at *n*xRev frequencies [15].

Finally, the crack breathing mechanism may occur. This consists of the cyclically opening and closing crack surfaces caused by the application of rotating bending. This phenomenon is illustrated

in Figure 1b: assuming the cracked rotor is rotating under the effect of a force that bends the axle downwards, compressive stresses are generated in the upper part of the axle section, whereas tensile stresses are generated in the lower part. Hence, when the crack is in the upper position, its surfaces are compressed so that the bending stiffness is the same or similar to that of a non-cracked section. When the crack moves to the lower position, the crack surfaces are separated resulting in a reduced bending stiffness. The breathing mechanism is therefore the result of the action of static loads (weight, reaction forces, etc.) and dynamical loads (i.e. unbalance, external excitation) combined with the axle rotation. Experimental results reported in [15] show that as long as static loads are predominant over the dynamic ones, the crack breathing is governed by the angular position of the shaft with respect to the stationary load direction. In this configuration, the crack opens and closes completely once per revolution.

Taking into consideration above-mentioned phenomena, the analysis of the different harmonic components in the cracked axle vibration signal provides opportunities for the detection of the crack itself. According to [15], when deflections are measured along the shaft loaded by its weight during a complete revolution of the shaft, the Fourier expansion allows the definition of 1xRev, 2xRev and 3xRev deflection shapes. Therefore, some typical symptoms of crack influence on shaft dynamic behaviour can be observed, namely a change in 1xRev, 2xRev and 3xRev vibration signal harmonics [16]-[19].

It should be noted that the above-mentioned results were obtained for industrial machinery and turbo-generators, for which the speed of revolution is often close or above the first critical, and the effect of external disturbances on the rotor is relatively limited, leading to a favourable signal-to-noise ratio in the analysis of *n*xRev vibration components. The aim of this paper is otherwise to investigate the feasibility of crack detection for a railway axle, considering the effect of disturbances arising from the interaction of the wheels with the rails and, particularly, the effect of wheel out-of-roundness, which represents an excitation phenomenon synchronous to the revolution of the axle.

3. Laboratory experiments

Full-scale fatigue durability tests were performed in the framework of the EURAXLES FP7 European Research Project [20] aimed at investigating fatigue strength for two different types of railway axles: hollow ones made of EA1N steel grade [21] and solid ones made of EA4T steel grade [21]. Thirteen axles were then tested to derive full-scale fatigue limits under constant amplitude loading by "stair case" sequences (assuming the "run-out" test at 10^7 cycles), so only some of the tested axles failed and developed fatigue cracks. Therefore, in this section, results will be shown only for five experiments: of these, four were stopped after the axle had developed a crack with significant size, whilst the other one ended with no crack. Table 1 summarizes the characteristics of the considered axles. As can be seen, a comprehensive range of the available cases was chosen, but it is worth remarking the different geometries, steels and loading conditions should not have an influence on the proposed SHM procedure, at least within their typical application in real axles.

3.1 Experimental set-up

The full-scale tests were performed using the Dynamic Test Bench for Railway Axles (fully compliant to EN 13261 [21] and quality certified ISO 17025) available at the labs of Politecnico di Milano, Department of Mechanical Engineering. This testing facility, shown in Figure 2, applies three-point rotating bending on a full-scale railway axle specimen. It consists of two supports carrying the axle through tapered bearing units and one central bearing unit connected to an actuator that applies a vertical load on the specimen under test. The specimen is set in rotation by an electric motor so to generate rotating bending fatigue. Both constant amplitude and block loading fatigue tests can be carried out as explained in [22] by setting a constant or variable load to be applied by the actuator.

In order to measure *n*xRev vibrations of the axle under test, an additional measuring set-up was introduced in the bench, consisting of three laser distance meters Mel Electronic M7L/20. Two laser transducers were mounted in vertical direction and one in horizontal direction, all pointing the central region of the axle (Fig. 3), which is the one undergoing the largest bending displacements so that the highest sensitivity for vibration changes was achieved. A 1xRev marker pulse (tacho signal) from the electric motor was used to trigger the acquisition of the signals from the laser transducers, ensuring synchronicity of these signals to the angular position of the crack. Finally, accelerometers were mounted on the test bench frame at laser transducers mounting locations, in order to take into account possible relative movements between the lasers and the axle, which would affect measurement accuracy.

3.2 Data acquisition and processing

Data acquisition was performed using a National Instrument cDAQ system. A sampling frequency of 10 kHz was chosen, to ensure that at least 1000 values per revolution were stored (the frequency of axle revolution in the tests was slightly below 10 Hz). Anti-aliasing digital filtering was performed using the internal functionalities of the cDAQ equipment.

Each 15 minutes, a record of data was automatically acquired and stored on a computer. The time record was then converted from the time domain to the angle domain and synchronous averaging of the signal over 100 revolutions was performed.

After synchronous averaging, the Fast Fourier Transform (FFT) algorithm was applied to extract the amplitude and phase of the *n*xRev components of the signal in frequency domain. Finally, trending analysis was applied mostly considering the trend with the progress of the test of the amplitude for the first seven *n*xRev components of axle vibration. The results of this analysis are presented in the next sub-section.

3.3 Experimental results

First, Figures 4a and 4b show the examples of final failures of test #1 and test #3 (Tab. 1). Cracks were detected, highlighted and sized, at least in terms of their surface length 2L, by colour-contrast magnetic testing (MT).

Figure 5 shows a comparison of the recorded axle vibration in a starting phase and in a more advanced stage taking, as an example, test #1 in which a crack initiated and then propagated. In particular, Figures 5a and 5c show the polar plots of the averaged measured vibration, whereas Figures 5b and 5d show the corresponding amplitudes of the *n*xRev components as obtained by the FFT analysis. The compared polar plots clearly show an increased asymmetry of the axle vibration in the final stage of the test, which is due to the asymmetric bending stiffness of the cracked rotor. The FFT analysis of the signals shows increased amplitudes of some harmonic components, especially the 1xRev and 2xRev, in the final stage of the test compared to the initial one. An analogous behaviour could be observed on the other considered failed axles.

The results of the trending analysis are shown in Figure 6 for test #1. In the plot, the amplitude of the first seven *n*xRev harmonics of vibration recorded during the test are plotted as a function of the number of loading cycles. The 1xRev, 2xRev and 3xRev harmonics show an increasing trend in the final part of the test, as expected. The trend of vibration with the cumulated cycles is sharply increasing in the final stage of the test: this means that the asymmetry and breathing effects, introduced by the crack, become more important after the crack has reached a significant size compared to the total resisting section A_{tot} of the axle, i.e. the total resisting area of the considered section in the axle when no crack is present. The amplitudes of the remaining 4xRev to 7xRev components remained very low during the test, with a slight increase in the final stage.

Unfortunately, direct measurements of crack size could not be carried out during the test, so a relationship between the amplitude of the *n*xRev harmonics and the size of the crack, cannot be straightforwardly established. However, the quantification, by colour-contrast MT, of the final surface length 2L allows estimating the final crack area *A* by means of the well-known and established crack propagation software AFGrow v. 4.0012.15 [23]: Figures 4c and 4d show the final

estimated crack shapes for tests #1 and #3, respectively: the estimated crack area A is the region in black colour Table 1 reports, then, the estimated A/A_{tot} ratio for each considered test: they resulted to be between 32% and 44% of the total resisting section of the axles, but it is worth remarking the first detected size of cracks must have been smaller. Moreover, as expected, different steel grades, geometries and load conditions seem to give a small influence on results.

Figure 7 compares the results of the trending analysis for the 1xRev (Fig. 7a) and 2xRev (Fig. 7b) harmonic components across the four tests ended in a crack propagation and for the one (test #5) in which no crack initiation occurred. A qualitatively similar trend is observed for tests #1-4, although the final amplitude of vibration is quite different. This can be explained noticing on one hand that the tests were carried out at different levels of applied constant amplitude rotating bending load and on the other hand that the final size of the crack was different for tests #1–#4. For test #5, the amplitude of the harmonic components (also those not shown in the figure) is approximately constant.

To finalize the SHM procedure, a warning criterion of cracked axle should be defined in order to promptly advise the operator about a likely imminent failure of an axle of the running train. A simple statistical approach is here proposed, considering the example case of 1xRev amplitudes during test #1. Such an approach is based on the approximately constant behaviour of "baseline" data before the final abrupt increase (Fig. 7). Figure 8a shows the statistical analysis of just these data, which seem to be reasonably described by a Normal distribution. The mean μ and the standard deviation σ of the distribution can then be determined and adopted to define the warning threshold. In particular, Figure 8b shows the mean level of the baseline data and the proposed threshold, as the 1xRev amplitude characterizing the 99% percentile $\mu+3\sigma$ of the baseline data themselves. This means that, when a 1xRev amplitude higher than the proposed threshold is acquired during service, the warning is issued. Applying the same procedure to all tests, it is possible to estimate that the warning would be issued between 96% and 98% of the lifetime, here intended as the number of fatigue cycles at which the given test was stopped.

To improve further the reliability of the warning procedure, some more actions could be taken. First, it can be easily applied to the other relevant *n*xRev amplitudes. Second, in order to decrease the probability of false calls, the warning could be issued only if two or three consecutive amplitudes exceed the warning threshold. Based on the analysis of experimental results presented in this section, it can be concluded that the 1xRev, 2xRev and 3xRev harmonic components of axle vibration contain information that can be useful for the structural health monitoring of railway axles. The 1xRev component shows the largest increase in amplitude at the final stage of the tests (and hence with the abrupt increase of the crack size). The amplitude of the 2xRev component is also sensitive to the number of load cycles. The 3xRev component shows a lower sensitivity to the number of load repetitions with a less clear trend, possibly because of disturbances such as thermal effects. It should be noted that, although the focus here is set on the amplitude of the *n*xRev harmonics, also phase information might be used to detect the presence of a fault. Some experimental results from a different application show a decrease in the amplitudes during the initial stage of crack development, which could be explained based on the phase shift between the pre-existing and additional vibration generated by crack growth [24].

4. Finite Element simulations

Numerical investigations were performed with the aim of investigating in more detail vibration effects induced by the presence of a crack in a rotating railway axle. To this aim, a Finite Element model of the cracked axle was defined using software ABAQUS v.6.12 [25]. Due to the non-linearity introduced by the crack, simulations were performed in time domain according to an explicit formulation.

Two simulation scenarios were considered: one aimed at reproducing the conditions of the laboratory tests presented in Section 3, the other aimed at reproducing the case of the axle being part of a railway wheelset running on a track.

4.1. Finite element model of a cracked axle

Based on the similarity between the scenarios considered in Table 1, a solid Finite Element model of the railway axle used in tests #1 and #2 was defined, i.e. a hollow configuration with 160 mm outer diameter and 65 mm bore diameter, which is typically used in passenger trains. Material data were set as linear elastic and according to the typical mechanical properties of EA1N railway steel grade.

The axle was discretised by means of iso-parametric hexahedral 8-node elements C3D8R with second-order interpolation and reduced integration. Because analyses were conducted by means of explicit method, the lumped mass formulation for all elements was applied to consider inertial effects involved in the simulation.

Cracks having semi-elliptical shape were considered. One single location of the crack was chosen: the same as in laboratory tests described in Section 3 and shown in Figure 4. Given that the crack breathing mechanism is the most important phenomenon to be investigated by the simulations, care was taken to ensure a proper behaviour of the Finite Element model in the cracked region. For this reason, a "surface to surface" type of contact was prescribed between crack surfaces [25]. The mono-lateral contact formulation was defined according to the "hard contact" pressure-overclosure model [25]: this is a penalty method that efficiently avoids interpenetration between the contacting surfaces, at the same time ensuring zero contact pressure when the surfaces of the crack are locally open. Isotropic friction with elastic regularisation was prescribed on the surfaces of the crack to reproduce tangential stresses generated in the contact area within the crack. The friction coefficient was set to 0.2 [15].

4.2 Simulation of laboratory tests

A first considered simulation scenario aims at reproducing the conditions of laboratory tests on the axle. Hence, suitable constraints were applied at the journal seats to reproduce the effect of the bearings supporting the axle in the test bench and the same load used in laboratory tests #2 (170 kN)

was applied as a distributed load acting in a central region of the axle having the same width as the wheel press-fit seat.

A rotational speed of 590 r.p.m. (the same as in laboratory tests) was considered. No external disturbances are considered in this simulation, so the whole vibration obtained is generated by the presence of the crack. The outputs considered for this simulation consist of the axle's bending deflection evaluated at the same locations where lasers transducers were placed in the laboratory tests. The conditions of this simulation scenario are shown in Figure 9a.

To investigate the influence of crack size on axle vibration, simulations were performed for different crack sizes in steps of 5% increase of crack area up to 45% of axle cross section, resulting in 10 different simulations. The time domain vibration signals obtained as outputs of the simulations were converted to the frequency domain by means of synchronous FFT, allowing the examination of the signals' harmonic components.

In Figure 10, the trends of the amplitude of the 1xRev, 2xRev and 3xRev harmonic components are presented as a function of cracked area of axle cross section. For crack areas up to 15% the amplitude of all considered components is very small, showing that the presence of a crack in this size range is not affecting significantly the axle's dynamic behaviour. For crack sizes in the range 15% to 30%, the amount of *n*xRev vibration starts to become significant and shows a slowly increasing trend with increasing crack size. For crack areas above 30%, the amplitude of vibrations generated by the crack is large and rapidly increasing with crack size, especially for 1xRev and 2xRev components.

Simulation results for the "laboratory tests" scenario appear to be in good agreement with the measurements performed in the full-scale tests on cracked axles presented in Section 3. In particular, the ratios of the amplitude for the 1xRev and 2xRev components shown in Figure 10 are in reasonable agreement with the ones obtained in laboratory tests. In particular, the amplitude of vibration obtained from Finite Element simulations, for crack sizes in the 32% – 35% range of axle

cross section, gets through to the amplitude of vibration obtained at the end of the laboratory tests, showing a fairly good agreement of test and simulation results.

Assuming, now, the numerical results for crack sizes up to 15% of axle cross section as baseline data (as mentioned above, the SHM procedure is insensitive within this range), the warning threshold was calculated for the example case of 1xRev components (detail in Figure 10). As can be seen, the SHM procedure issues a likely failure warning for a crack area equal to about 16% of axle cross section, which corresponds, for the considered case of hollow axle, to 2670 mm^2.

This result allows estimating the residual lifetime of the axle, an information useful to understand if the train must be immediately stopped on the track and the axle itself substituted, or if there is a possibility to reach the nearest railway station without closing down the line. The calculation was carried out, again, by means of the dedicated AFGrow software package. In particular:

- the geometry of the analysed axle is the same of FEM simulations (see section 4.1);
- the initial crack size is equal to 16% of axle cross section, while the final one is assumed as in test #2;
- a simple crack growth algorithm, not able to keep into account load interaction effects, was adopted;
- a typical in-service load spectrum [26], representative of about 57000 km of high-speed service, was adopted;
- crack growth properties for EA1N steel were previously derived [27].

The crack propagation simulation highlighted that, to go from 16% to 32 % of axle cross section, 85000 km are needed, suggesting the possibility to reach the nearest railway station for maintenance without closing down the line. It is worth remarking this scenario is valid just for the considered case, any other one needs new analyses. Moreover, the possibility to detect the 16% fracture of axle cross section was determined by the quasi-ideal scenario of a lab, while more disturbing effects take place on real tracks, as described in the following sub-section.

4.3 Simulation of the axle running on a railway track

The second simulation scenario considers the axle as part of a railway wheelset running at constant speed over a railway track. In this case, two static forces of intensity 85 kN are applied at the axle-box seats and are reacted by constraints applied on the wheel press-fit seats, reproducing a total axle load of 170 kN. The rotational speed considered for the axle is again 590 r.p.m., corresponding to a forward speed of the wheelset of 100 km/h. All simulations were performed considering a crack area A equal to 35% of the total axle cross section A_{tot}: this is a very large crack that would require the axle to be put immediately out of service

In this simulation, the additional excitation of axle vibration, due to wheel out-of-roundness and track irregularity, was considered by applying time varying displacements at the two wheel seats. The conditions of this simulation scenario are shown in Figure 9b.

Special interest was paid to wheel out-of-roundness (OOR) excitation, as this gives rise to excitations having the same periodicity (nxRev) as the crack breathing mechanism. A profile of wheel out-of-roundness was introduced as a sum of twenty sine functions with wavelengths corresponding to the nominal wheel circumference (2.88 m) and the nineteen lowest sub-multiples. The amplitudes of these components were defined based on the elaboration of experimental measurements of wheel OOR provided in [28] and the phases were randomly generated. Two levels of wheel OOR are considered: the first one, referred to as “new wheel OOR”, is typical for a new or recently re-profiled wheel. The second level, named “worn wheel OOR” is representative of a long serviced wheel, close to being in need of re-profiling. Track irregularity was introduced using some spatial realisations available from software SIMPACK [29]. The profiles of wheel OOR and track irregularity were summed to produce a single time history of the displacements applied at the two wheel seats of the FE model.

For this second scenario, six simulations are considered: cases n. 1–3 assume no crack is present in the axle and consider the effect of a new wheel OOR profile, worn wheel OOR and worn wheel

OOR combined with track irregularity, respectively. Cases n. 4–6 replicate the previous ones considering, in addition, the presence of a crack area corresponding to 35% of axle cross section. Table 2 resumes the amplitude of the 1xRev, 2xRev and 3xRev harmonics obtained for these cases (values are reported in μm): as expected when no crack is present, significant *n*xRev vibration is obtained for cases considering the presence of severe wheel OOR. Compared to the presence of wheel OOR only (case n. 2), the additional consideration of track irregularity (case n. 3) produces minor variations especially for the 2xRev and 3xRev harmonics: this is justified by the fact that track irregularity represents a broadband random excitation occurring at wavelengths not especially related with the wheel circumference.

As far as cases n. 4–6 are concerned, the additional presence of the crack produces a very significant increase of the 1xRev and 2xRev harmonics, whereas the 3xRev one is less influenced. The amplitude of the 1xRev component in cases n. 4 and 5 is more than two times larger than any other case run for an axle with no crack. In case n.6, the one also including track irregularity, the amplitude of the 1xRev harmonic is lower than for cases n. 4 and 5, but this could be due to the particular spatial realisation of track irregularity used in the simulation: this issue is worth of further investigation. The 2xRev component is very highly affected by the presence of the crack and the amplitude obtained in cases n. 4–6 is six to seven times larger than the one obtained when no crack is present.

It can be then concluded the increase of 1xRev and especially 2xRev vibration occurring in a cracked axle is sufficient to diagnose the presence of the crack. Of course, this conclusion depends on the assumed size of the crack: in the investigation presented here, the assumed size, together with the final A/A_{tot} values shown in Table 1, requires the cracked axle is immediately removed from service. It is also worth emphasising that the model assumed in this scenario is quite simplified compared to the case of a real wheelset running on a track: in particular, the effects of track flexibility and wheel conicity are not considered here. A more detailed investigation of this scenario is envisaged as a next step of the research.

5. Conclusions

In this paper, a method for the structural health monitoring of railway axles was presented. The method aims at identifying the presence of a crack in the axle based on measuring the axle's bending vibration. Crack detection is achieved through the examination of the *n*xRev harmonic components in the axle bending vibration, i.e. vibration components having periodicity which is an integer sub-multiple of the axle revolution period, that are induced by the so called crack-breathing mechanism and by asymmetry in the bending stress of the axle, as produced by a propagating crack.

The feasibility of this monitoring approach was initially investigated by means of experiments performed on a laboratory test rig and demonstrated to be a promising method for railway axles crack monitoring application. In particular, a clear trend of some *n*xRev vibration components was observed to be associated with an increase in the size of the propagating crack. The *n*xRev components that proved to be more suitable for crack detection are the 1xRev, 2xRev and 3xRev. A simple, but effective, statistical method for the definition of a warning threshold to stop the train before failure is proposed, as well.

Numerical investigations were performed to investigate the feasibility of the monitoring approach in a real service condition, especially looking at the effect of disturbances caused by wheel out-of-roundness and track irregularity. To this aim, a Finite Element model of the cracked axle was defined considering different crack depths and shapes. Due to the non-linearities introduced by the crack, simulations were performed in time domain according to an explicit formulation.

In the first stage, boundary and load conditions were defined to reproduce the laboratory tests performed and the model was found to provide results that are in fairly good agreement with the tests. Then different boundary and load conditions were applied to reproduce the case of a railway wheelset running on the track. It was found that, despite the effect of disturbances generated by wheel out-of-roundness and track irregularity, the presence of a crack area of 35% of axle cross

section produces a significant amount of additional 1xRev and 2xRev vibration compared to a non-cracked axle, thereby showing the possibility of using this kind of measurement for the monitoring of the axle's structural integrity in a real application.

Future investigations will look at the effect of the location of the crack in the axle, defining a suitable measuring set-up for the on-track application of the method. Furthermore, measurements are foreseen to be performed on a roller rig using a cracked axle, to investigate experimentally the sensitiveness and accuracy of the method considering all the disturbance effects related to wheel-rail interaction.

Acknowledgements

The SHM results were obtained in the frame of the SUSTRAIL Collaborative European Project (Grant Agreement #265740). The full-scale fatigue tests were performed in the frame of the EURAXLES Collaborative European Project (Grant Agreement #265706). The authors would like to thank Prof. S. Beretta (Dept. Mechanical Engineering, Politecnico di Milano) for the useful help and discussions.

References

[1] A. Orlova, Y. Boronenko, The Anatomy of Railway vehicle Running Gear, in Iwnicki S. Ed. "Handbook of Railway Vehicle Dynamics", 2006, Taylor & Francis.

[2] Hoddinot DS. Railway axle failure investigations and fatigue crack growth monitoring of an axle. J Rail Rapid Transit 2004;218:283–92.

[3] Beretta S, Carboni M, Lo Conte A, Palermo E. An investigation of the effects of corrosion on the fatigue strength of A1N axle steel. J Rail Rapid Transit 2008;222:129–43.

[4] Gravier N, Viet JJ, Leluan A. Prédiction de la durée se vie des essieux-axes ferroviaires. Revue générale des chemins de fer 1999;3:33–40.

[5] EN 13103:2012: Railway Applications – Wheelset and Bogies – Non-powered axles – Design Method, European Committee for Standardization, Technical Committee CEN/TC 25, 2012.

[6] EN 13104:2012: Railway Applications – Wheelset and Bogies – Powered axles – Design Method, European Committee for Standardization, Technical Committee CEN/TC 25, 2012.

[7] Grandt AF Jr, Fundamentals of Structural Integrity, JohnWiley & Sons, Hoboken, NJ, 2004.

[8] Zerbst U, Beretta S, Köhler G, Lawton A, Vormwald M, Beier HTh, Klinger C, Černý I, Rudlin J, Heckel T, Klingbeil D. Safe life and damage tolerance aspects of railway axles - A review. Engineering Fracture Mechanics 2013, 98: 214-271.

[9] Cantini S, Beretta S (Editors), Structural reliability assessment of railway axles, LRS-Techno Series 4, 2011.

[10] S. Y. Chong, J. R. Lee and H. J. Shin, A review of health and operation monitoring technologies for trains, Smart Structures and Systems, Vol. 6, No. 9 (2010) 1079-1105.

[11] C. H. Jiang, W You, L. S. Wang, M. Chu, N. Zhai, Real-time monitoring of axle fracture of railway vehicles by translation invariant wavelet, Proceedings of 2005 International Conference on Machine Learning and Cybernetics, Vols 1-9 pp. 2409-2413.

[12] C. H. Jiang, A fault diagnosis system of railway vehicles axle based on translation invariant wavelet, Proceedings of 2007 International Conference on Machine Learning and Cybernetics, Vols 1-7 Pages: 1045-1050.

[13] S. Bruni, M. Carboni, D. Crivelli, M. Guagliano, and P. Rolek, (2013) A preliminary analysis about the application of acoustic emission and low frequency vibration methods to the structural health monitoring of railway axles, Chemical Engineering, vol. 33, 697-702.

[14] http://www.sustrail.eu/, accessed on April 2015.

[15] N. Bachschmid, P. Pennacchi, and E. Tanzi, Cracked rotors: a survey on static and dynamic behaviour including modelling and diagnosis: Springer Science & Business Media, 2010.

[16] I. Imam, S. Azzaro, R. Bankert, and J. Scheibel, "Development of an on-line rotor crack detection and monitoring system," Journal of Vibration and Acoustics, vol. 111, pp. 241-250, 1989.

[17] T. Zhou, Z. Sun, J. Xu, and W. Han, "Experimental analysis of cracked rotor," Journal of dynamic systems, measurement, and control, vol. 127, pp. 313-320, 2005.

[18] J.-J. Sinou and A. Lees, "The influence of cracks in rotating shafts," Journal of Sound and Vibration, vol. 285, pp. 1015-1037, 2005.

[19] O. Jun, H. Eun, Y. Earmme, and C.-W. Lee, "Modelling and vibration analysis of a simple rotor with a breathing crack," Journal of Sound and vibration, vol. 155, pp. 273-290, 1992.

[20] http://www.euraxles.eu/, accessed on April 2015.

[21] EN 13261: Railway Application – Wheelsets and Bogies – Axles – Product Requirements, European Committee for Standardization, Technical Committee CEN/TC 25, 2011.

[22] Beretta S., Carboni M.: Variable amplitude fatigue crack growth in a mild steel for railway axles: experiments and predictive models, Eng. Fract. Mech., Vol. 78, 2011, 848-862.

[23] AFGROW v. 4.0012.15. User's Manual, 2008.

[24] R. B. Randall, Vibration-based condition monitoring: industrial, aerospace and automotive applications: John Wiley & Sons, 2011.

[25] "ABAQUS/Explicit (version 6.12) User's Manual (2012)," ed: Dassault Systemes.

[26] Beretta S, Carboni M, Cervello S. Design review of a freight railway axle: fatigue damage versus damage tolerance. Mat-Wiss U Werkstofftech 2011;42.

[27] Carboni M., Beretta S., Madia M. (2008), Analysis of crack growth at R=-1 under variable amplitude loading on a steel for railway axles, J. ASTM Int. 5(7), 1-13.

[28] Nielsen J. C. O. and Johansson A., Out-of-round railway wheels – a literature survey, Proceedings of the Institution of Mechanical Engineers, Part F: Journal of Rail and Rapid Transit, Vol. 214, pp. 79-91, 2000.

[29] Schupp G., Netter H., Mauer L., Gretzschel M., Multibody System Simulation of Railway Vehicles with SIMPACK, Vehicle System Dynamics Vol. 31 S, pp. 104-118, 1999.

LIST OF TABLES

Test #	**Axle type**	**Monitored diameter (D) [mm]**	**Cycles to failure**	**Final crack surface length (2L) [mm]**	**Estimated final crack area (A) [mm^2]**	**A/A_{tot} [%]**
1	EA1N, hollow	160	3909431	175	5845	35
2	EA1N, hollow	160	3613110	166	5344	32
3	EA4T, solid	147	2620000	170	5613	33
4	EA4T, solid	147	989134	200	7410	44
5	EA4T, solid	Reference case: no crack and no failure after 10^7 fatigue cycles				

Tab. 1

Case n.	35% crack	Wheel OOR	Track irregularity	Amplitude 1xRev [µm]	Amplitude 2xRev [µm]	Amplitude 3xRev [µm]
1	No	New	No	12	2	3
2	No	Worn	No	100	23	75
3	No	Worn	Yes	126	22	70
4	Yes	New	No	280	130	30
5	Yes	Worn	No	260	130	50
6	Yes	Worn	Yes	198	133	75

Tab. 2

LIST OF FIGURES

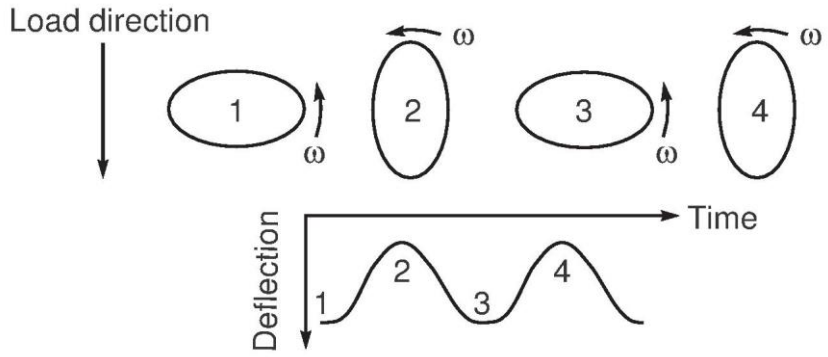
Load direction
ω
ω
1
2
3
4
ω
ω
Time
Deflection
1
2
3
4

(a)

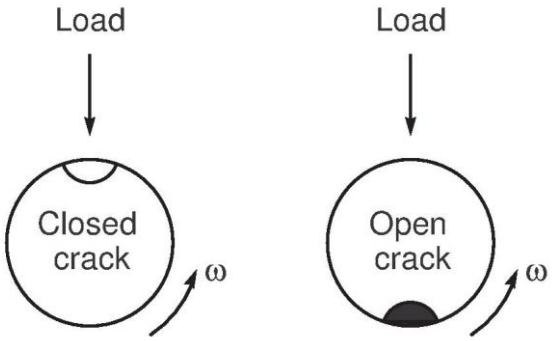
Load
Load
Closed crack
Open crack
ω
ω

(b)

Fig. 1

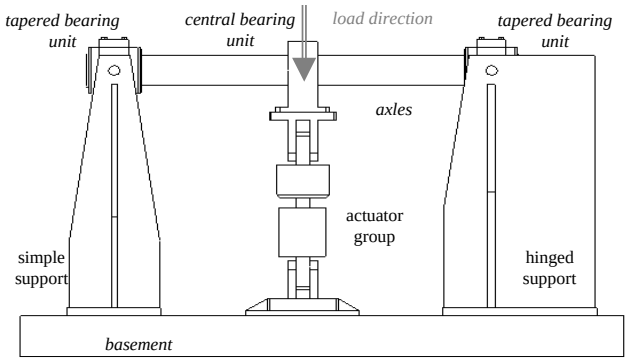
tapered bearing unit
central bearing unit
load direction
tapered bearing unit
axles
actuator group
simple support
hinged support
basement

(a)

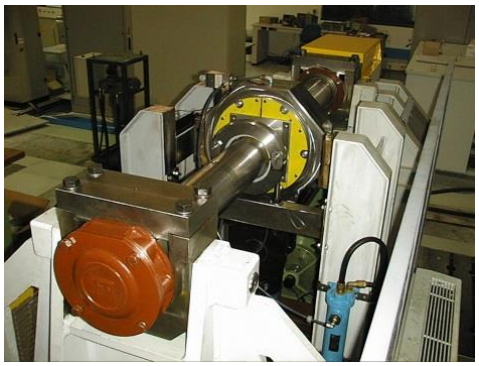

(b)

Fig. 2

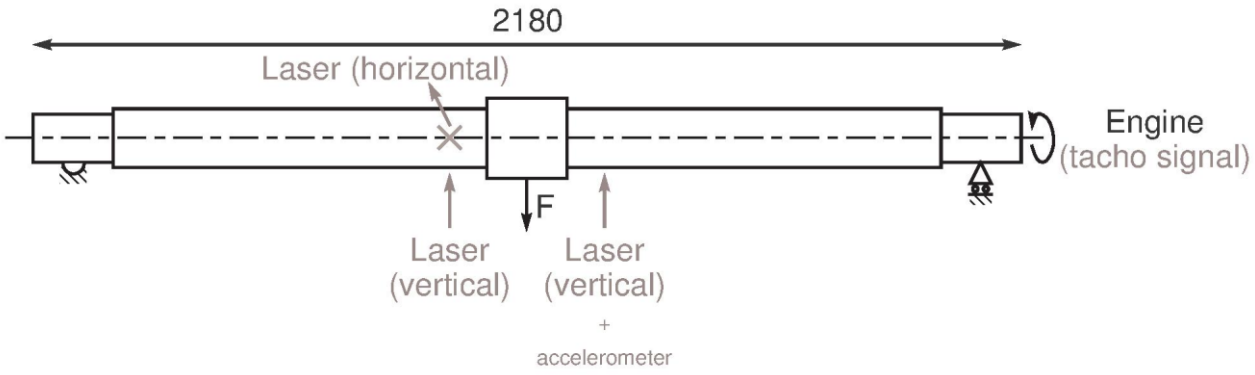
2180
Laser (horizontal)
Engine
(tacho signal)
F
Laser
(vertical)
Laser
(vertical)
+
accelerometer

Fig. 3

(a)

(b)

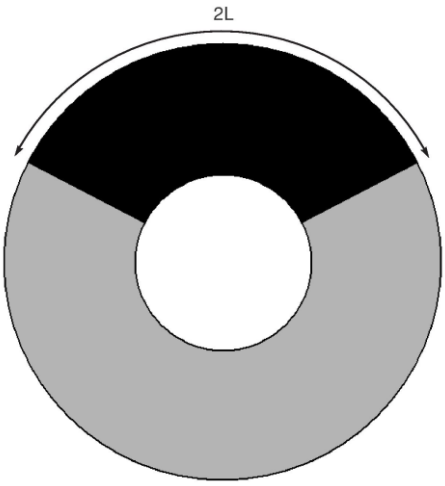

(c)

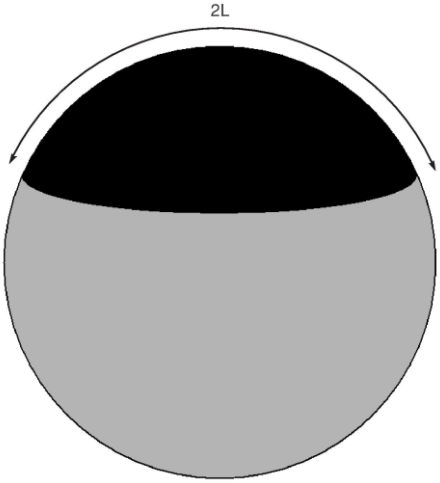

(d)

Fig. 4

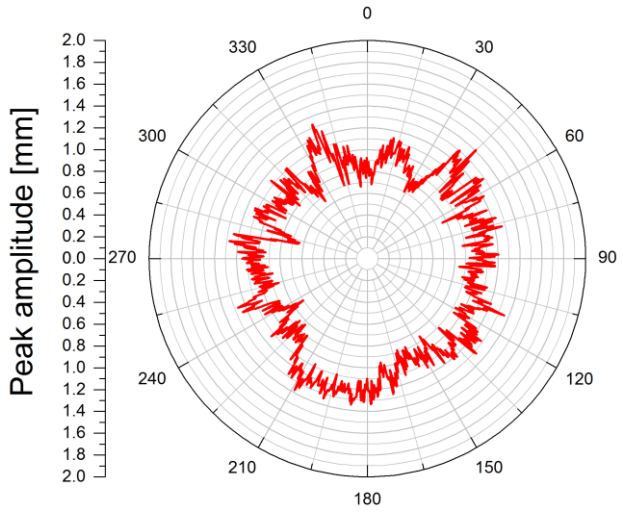
Peak amplitude [mm]
0
30
60
90
120
150
180
210
240
270
300
330
2.0
1.8
1.6
1.4
1.2
1.0
0.8
0.6
0.4
0.2
0.0

(a)

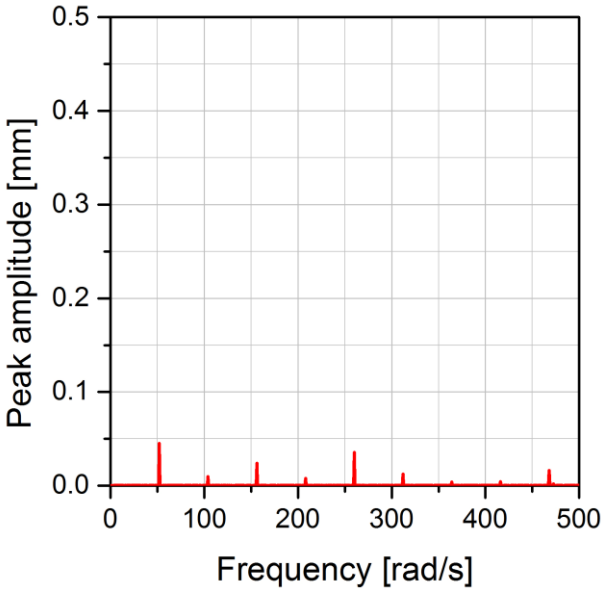
Peak amplitude [mm]
Frequency [rad/s]
0.5
0.4
0.3
0.2
0.1
0.0
0
100
200
300
400
500

(b)

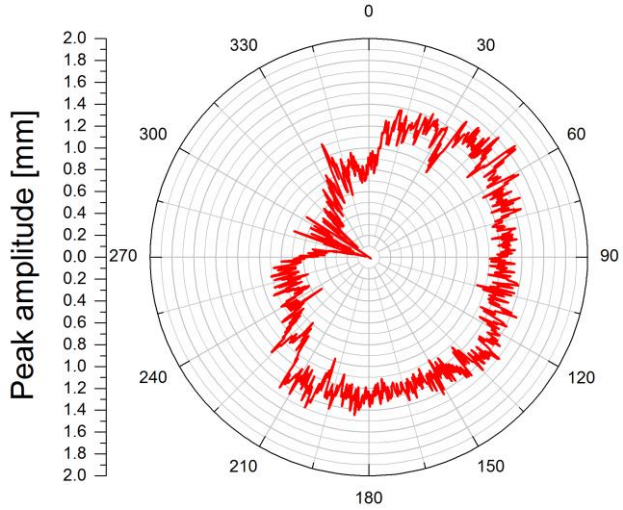
Peak amplitude [mm]
0
30
60
90
120
150
180
210
240
270
300
330
2.0
1.8
1.6
1.4
1.2
1.0
0.8
0.6
0.4
0.2
0.0

(c)

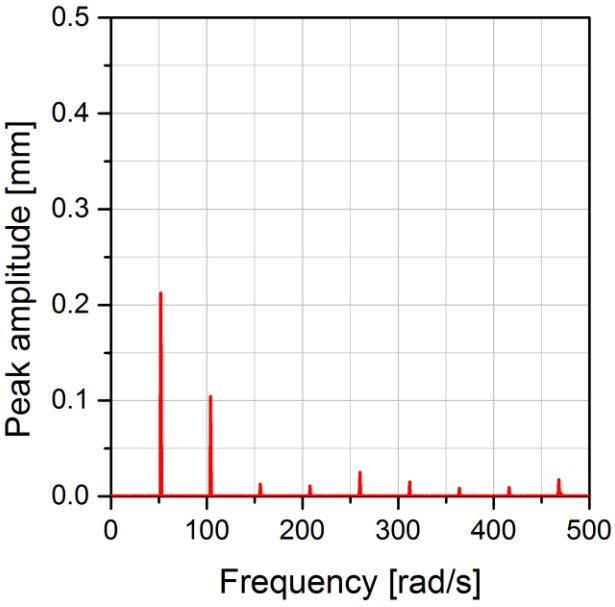
Peak amplitude [mm]
Frequency [rad/s]
0.5
0.4
0.3
0.2
0.1
0.0
0
100
200
300
400
500

(d)

Fig. 5

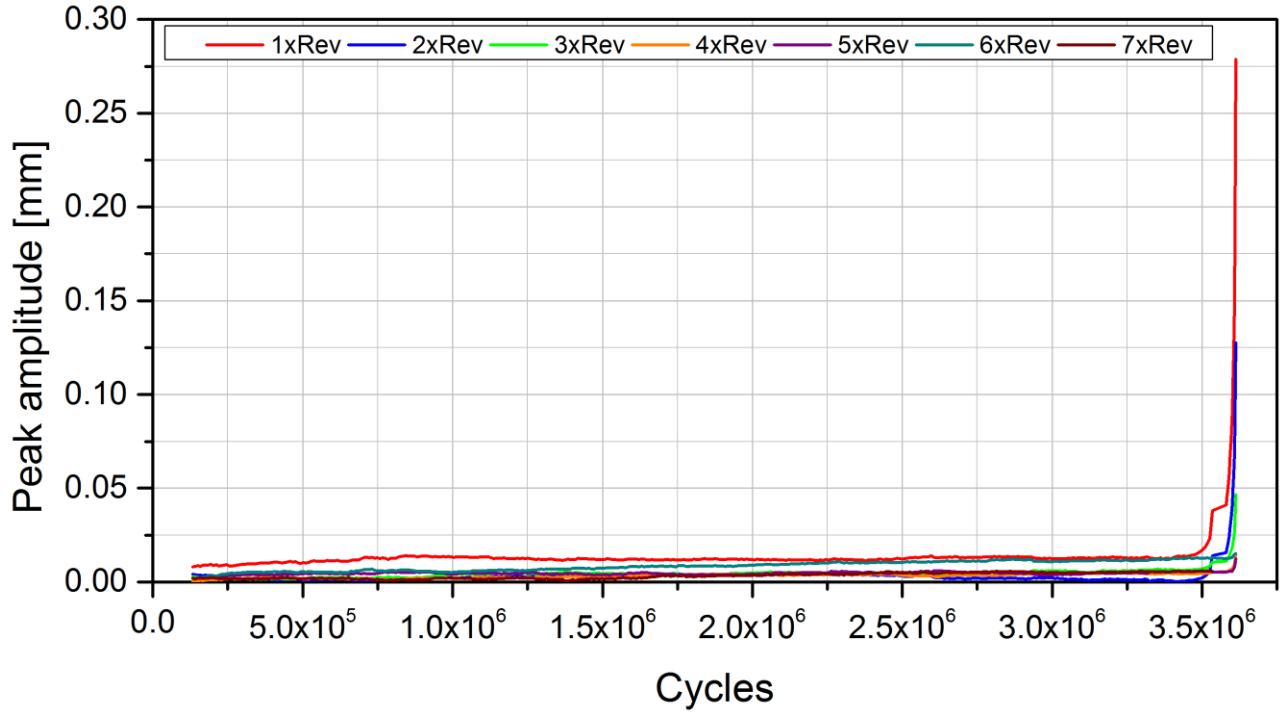
1xRev
2xRev
3xRev
4xRev
5xRev
6xRev
7xRev
Peak amplitude [mm]
0.30
0.25
0.20
0.15
0.10
0.05
0.00
0.0
5.0x10^5
1.0x10^6
1.5x10^6
2.0x10^6
2.5x10^6
3.0x10^6
3.5x10^6
Cycles

Fig. 6

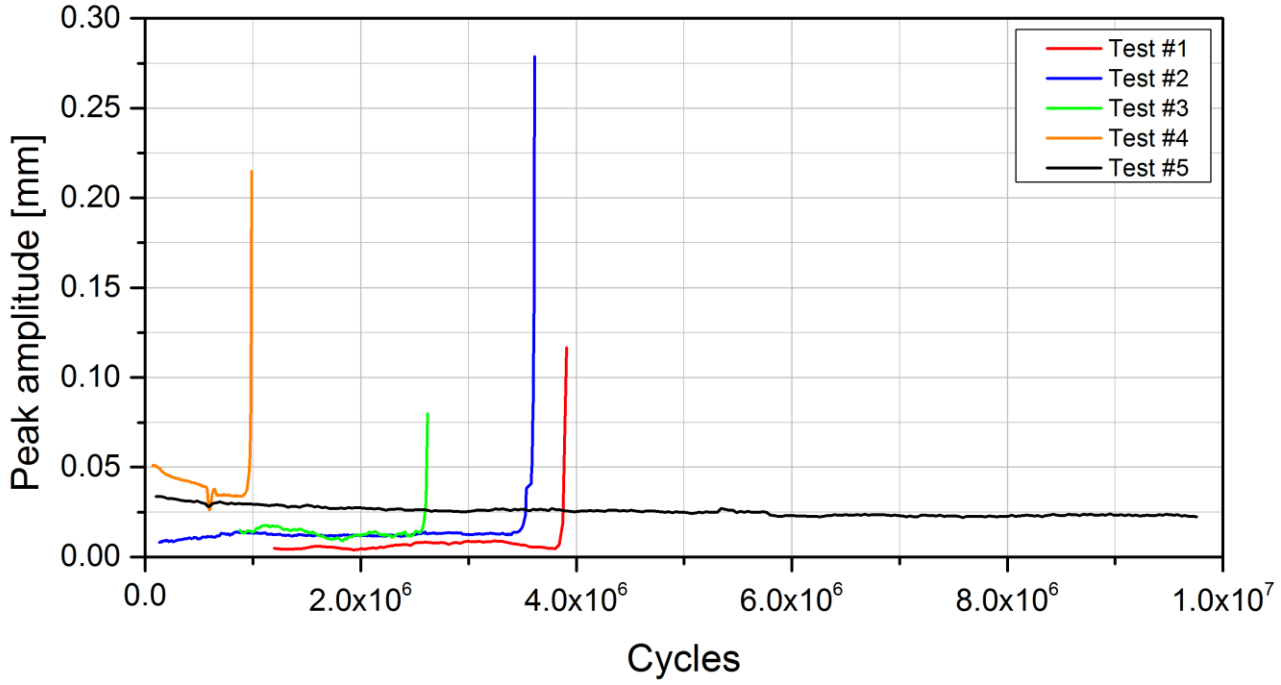
Peak amplitude [mm]
0.30
0.25
0.20
0.15
0.10
0.05
0.00
0.0
2.0x10^6
4.0x10^6
6.0x10^6
8.0x10^6
1.0x10^7
Cycles
Test #1
Test #2
Test #3
Test #4
Test #5

(a)

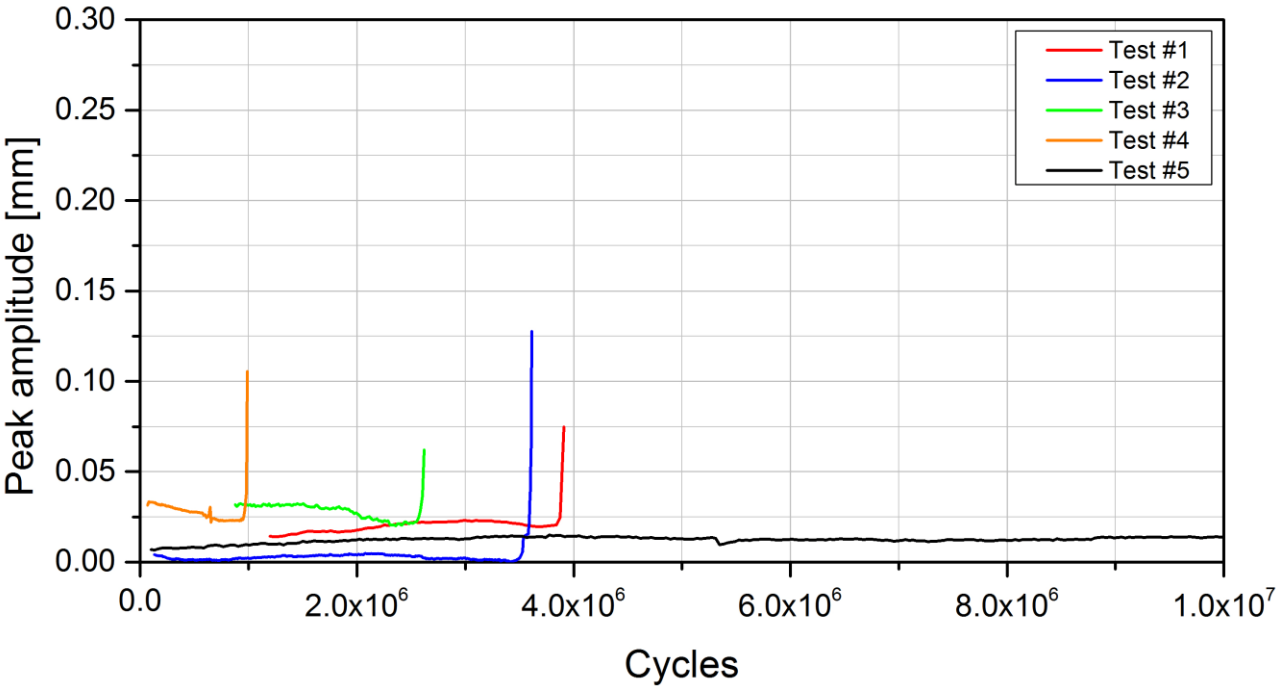
Peak amplitude [mm]
0.30
0.25
0.20
0.15
0.10
0.05
0.00
0.0
2.0x10^6
4.0x10^6
6.0x10^6
8.0x10^6
1.0x10^7
Cycles
Test #1
Test #2
Test #3
Test #4
Test #5

(b)

Fig. 7

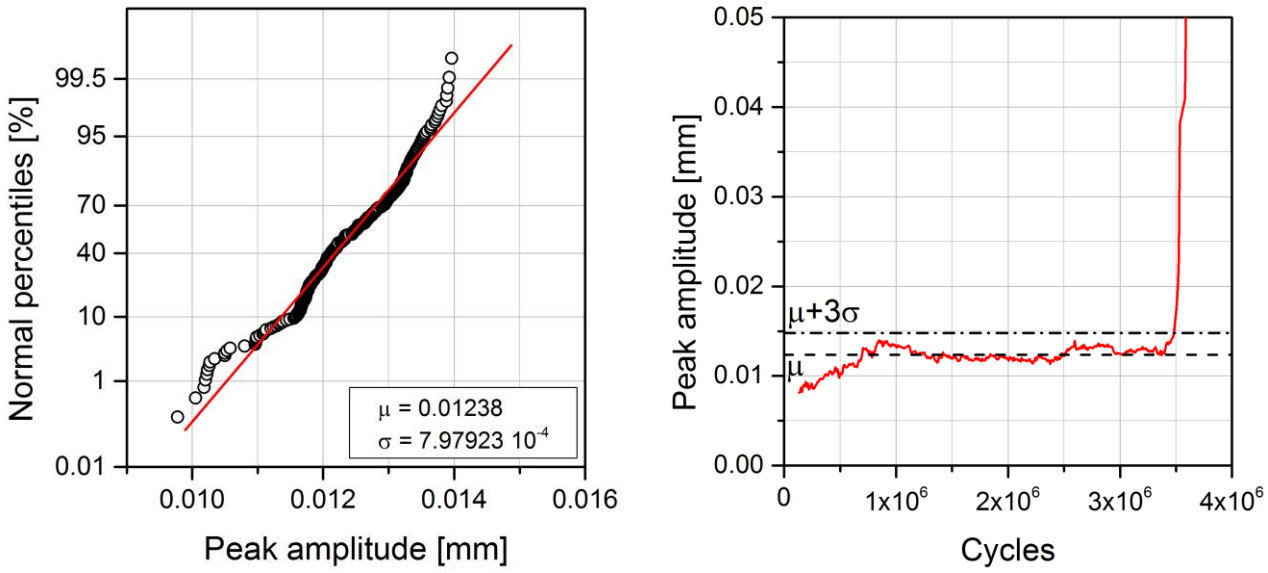
Normal percentiles [%]
99.5
95
70
40
10
1
0.01
0.010
0.012
0.014
0.016
Peak amplitude [mm]
μ = 0.01238
σ = 7.97923 10-4
Peak amplitude [mm]
0.05
0.04
0.03
0.02
0.01
0.00
μ+3σ
μ
0
1x10^6
2x10^6
3x10^6
4x10^6
Cycles

(a) (b)

Fig. 8

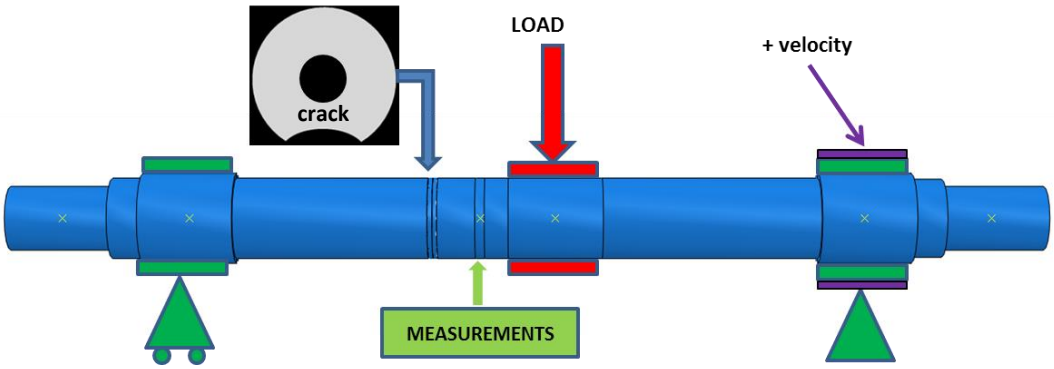
LOAD
+ velocity
crack
MEASUREMENTS

(a)

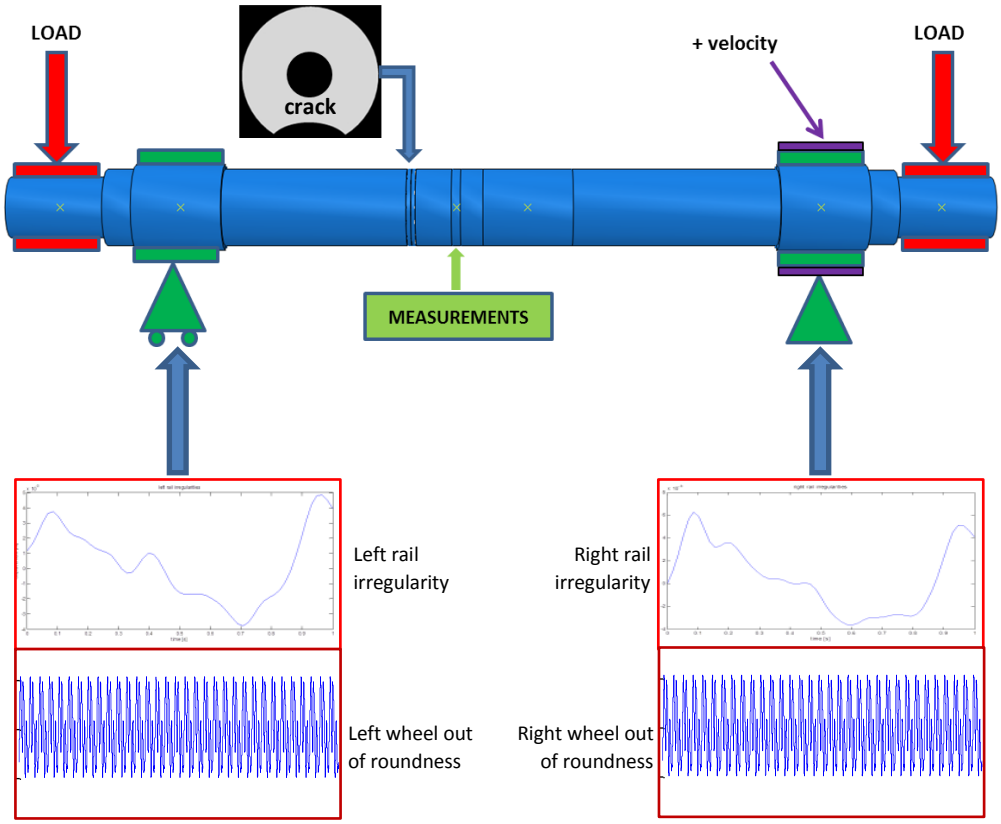
LOAD
crack
+ velocity
LOAD
MEASUREMENTS
Left rail irregularity
Right rail irregularity
Left wheel out of roundness
Right wheel out of roundness

(b)

Fig. 9

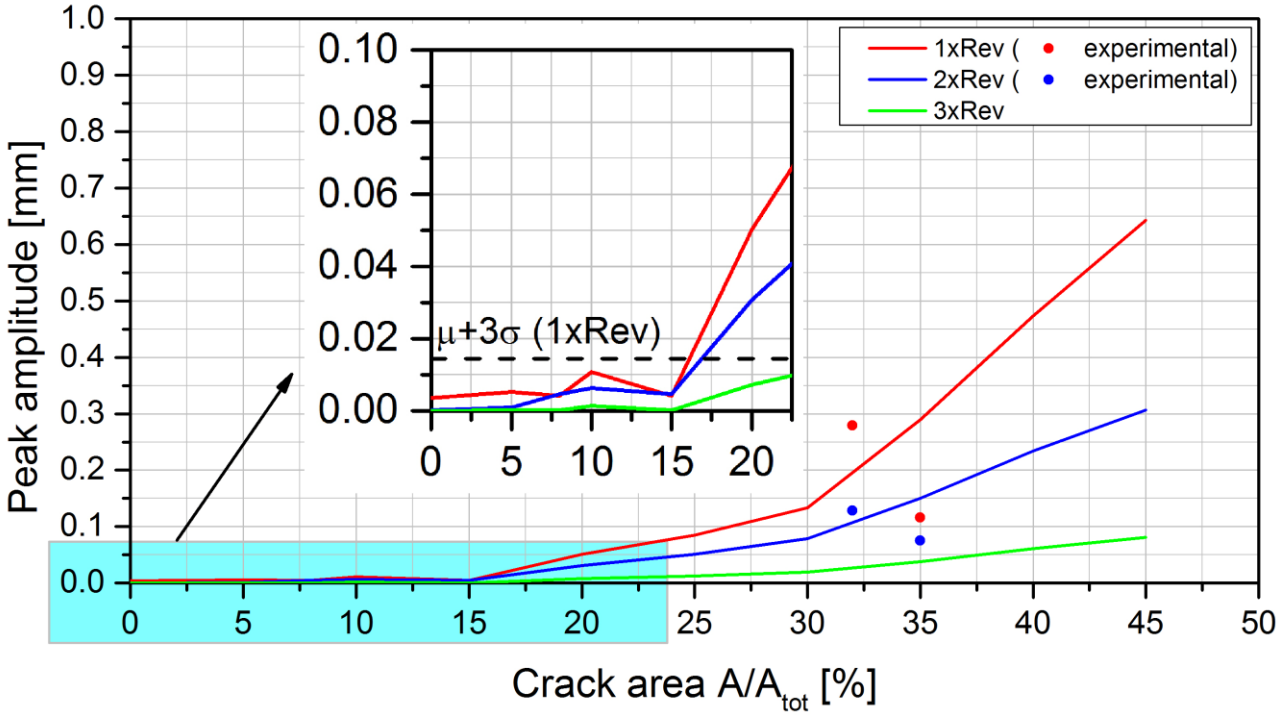
Peak amplitude [mm]
Crack area A/A$_{tot}$ [%]
1xRev (experimental)
2xRev (experimental)
3xRev
μ+3σ (1xRev)

Fig. 10